Synthesis of ZnO Nanobelts by Carbothermal Reduction and Their Photoluminescence Properties

Xianghua Kong, Xiaoming Sun, and Yadong Li*
Department of Chemistry and the Key Laboratory of Atomic & Molecular Nanoscience
(China Ministry of Education), Tsinghua University, Beijing 100084, P. R. China

(Received November 22, 2002; CL-020994)

Semiconducting ZnO nanobelts have been fabricated by carbothermal reduction process using ZnO powders mixed with graphite as starting materials at a temperature of 900 °C. SEM, TEM images and SAED show that the nanobelts are pure, thin, uniform, and single-crystalline. One strong green-light emission peak at 500 nm was observed.

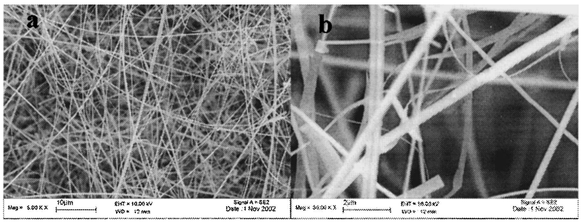

Figure 1. (a) A typical SEM image of the as-prepared nanobelts obtained 600 °C. (b) Typical high-magnification SEM images of the nanobelts.

ZnO is an important semiconductor material and has been used widely for its catalytic, electrical, optoelectronic and photochemical properties.[1] Because of its wide direct band gap (3.37 eV) and large exciton binding energy (60 meV) at room temperature, it has been recognized as one of the promising photoelectronic materials in the blue-ultraviolet region.[2] It is predicted that the photo-to-electron conversion efficiency, gas sensing and photonic performance would be enhanced by reducing the dimension of ZnO structure because of surface area increase and quantum confinement effect.[3] The room temperature ultraviolet lasting in ZnO nanowires arrays has been demonstrated.[4] One-dimensional (1D) ZnO nanostrutures including nanowires, nanorods, and multipods have been synthesized by various technique.[5–8] Recently, it was reported that physical evaporation of ZnO powders at high temperature resulted in the formation of ZnO nanobelts.[9,10] However, it is difficult to directly synthesize the nanobelts by simply evaporating ZnO powder because it requires higher processing temperature (above 1300 °C). So how to get ZnO nanobelts with high purity at relatively low temperature is quite important. In this paper, a simple and high-yield method was developed for fabrication of ZnO nanobelts starting from ZnO powders mixed with graphite.

ZnO powders mixed with graphite (molar ratio 1:1) was used as source material. The reaction system consists of a horizontal tube furnace and quartz tube. The source materials were placed at the center of an alumina crucible, and the crucible was inserted into the center of quartz tube in a horizontal tube furnace. Several alumina plates were placed downstream one by one acted as the collectors. The temperature of crucible was increased to 900 °C in one hour and was kept at 900 °C for 30 min. under a constant flow of argon at rates of 200 standard cubic centimeters per minute (sccm). White products were formed in the region downstream from the higher temperature zone with a temperature of about 600 °C. The as-prepared products were characterized and analyzed by scanning electron microscopy (SEM) (LEO-1530), X-ray diffraction (XRD) (Bruker D8 advance), and transmission electron microscopy (TEM) (Hitachi, H-800 at 200 kV). The PL measurements were carried out on a PERKIN ELMER LS50B UV-visible spectrophotometer at room temperature.

A typical SEM image for the products is shown in Figure 1a. The image shows that a large quantity of wirelike nanostructures were formed. Their length ranges from several tens to several hundreds of micrometers; some of them even have lengths on the order of millimeter. Figure 1b exhibits magnified SEM images of the products. It can be seen that the products show beltlike morphology. The typical widths of the nanobelts are in the range of several tens to several hundreds nanometer. XRD patterns from the as-synthesized nanobelts samples show that all of the diffraction peaks can be indexed to the hexagonal structure of ZnO (XRD support). No diffraction peaks from Zn or other impurities have been found.

The typical TEM image of the as-prepared products was shown in Figure 2. The lengths of the nanobelts were up to several hundreds of micrometers. Each nanobelt has a uniform width and thickness along its entire length. Figure 2 displays a bent ZnO nanobelt, which exhibited a thickness no more than 50 nm. The typical widths of the nanobelts are in the range of 30–300 nm. The growth directions for the nanobelts were determined from the SAED patterns inset in Figure 2. It demonstrated that this particular nanobelt was a single crystal with a growth direction of [$01\bar{1}0$], other than [0001] like ZnO nanowires.[5]

From the SEM and TEM results, it can be found that the purity of ZnO nanobelts is very high, no particles, nanowires

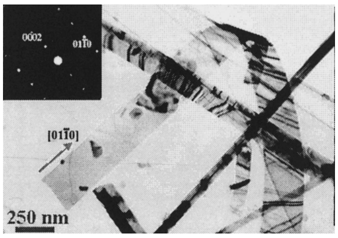

Figure 2. A TEM image of an individual ZnO nanobelt. Inset was the SAED patterns of the nanobelt.

and other structures were found. The yield of products was 20–30%, according to the amount of ZnO used. In our experiment, we also found that the width of ZnO nanobelts was sensitive to the flow rate of carrying gas (argon). When the flow rate was decreased, ZnO nanobelts would grow in higher temperature region, and the size of ZnO nanobelts would increase markedly. For example, when the flow rate of argon decreased to 10 sccm, the ZnO nanobelts were obtained at 850 °C, the width of ZnO nanobelts is about 20 um. (SEM support). So the size could be manipulated in this way.

At high temperature, carbon reduced ZnO into Zn by the following reactions:[4,5,11]

$$\mathrm{ZnO} + \mathrm{C} \rightarrow \mathrm{Zn} + \mathrm{CO_2}, \qquad (1)$$

$$\mathrm{C} + \mathrm{CO_2} \rightarrow \mathrm{CO}, \qquad (2)$$

$$\mathrm{ZnO} + \mathrm{CO} = \mathrm{Zn}\ (\mathrm{g}) + \mathrm{CO_2}. \qquad (3)$$

At equilibrium state, reaction (1) is difficult to occur because Zn metal has a high vapor pressure at high temperature. However in our system the reaction can proceed as equation (1) by the important role of Ar flow. When Zn vapor occured, the Zn vapor was quickly brought to the low temperature region downstream of the quartz tube by Ar, the Zn pressure at the source place would decrease to a relative low level, thus reaction (1) can occur continuously. The Zn vapor, CO and $\mathrm{CO_2}$ were transported to the low temperature region downstream of the quartz tube, then the Zn vapor would be oxidized into ZnO again:[5]

$$\mathrm{Zn}\ (\mathrm{g}) + \mathrm{CO_2} = \mathrm{ZnO} + \mathrm{CO}. \qquad (4)$$

Figure 3 illustrates the room temperature photoluminescence (PL) spectra recorded for the as-prepared ZnO nanobelts. A UV emission at 380 nm and a strong green emission at 500 nm were detected. UV band emission of ZnO has been well understood to be related to the exciton emission.[10] Vanheusden and co-workers proved that the singly ionized oxygen vacancies are responsible for the green emission and the emission results from the recombination of a photogenerated hole with an electron occupying the oxygen vacancy.[12] It is well-known that surface states may seriously influence the PL process in nanomaterials. It has been reported that the progressive increase of the green light emission intensity relative to the UV emission is observed as the wire diameter decreases, which suggests that there is a great fraction of oxygen vacancies in the nanowires.[5] In our work, the as-prepared nanobelts are very thin, so we believe that these nanobelts with high aspect ratios should have more surface and subsurface oxygen vacancies. Therefore, it was reasonable to explain that the green-light emission from the ZnO nanobelts could be attributed to the singly ionized oxygen vacancies.

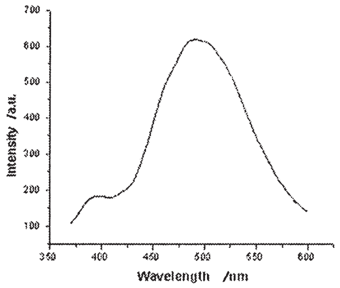

Figure 3. PL spectrum of the ZnO nanobelts at room temperature.

This work was supported by NSFC (20025102, 50028201, 20151001) and the state key project of fundamental research for nanomaterials and nanostructures.

References

1 L. Vayssieres, K. Keis, A. Hagfeldt, and S. E. Lindquist, *Chem. Mater.*, **13**, 4386 (2001).
2 Y. Chen, D. M. Bagnall, H. Koh, K. Park, K. Hiraga, Z. Zhu, and T. Yao, *J. Appl. Phys.*, **84**, 3912 (1998).
3 R. F. Severse, *Science*, **276**, 895 (1997).
4 M. H. Huang, S. Mao, H. Feick, H. Q. Yan, Y. Y. Wu, H. Kind, E. Weber, R. Russo, and P. D. Yang, *Science*, **292**, 1897 (2001).
5 M. H. Huang, Y. Y. Wu, H. N. Feick, N. Tran, E. Weber, and P. D. Yang, *Adv. Mater.*, **13**, 113 (2001).
6 Y. C. Kong, D. P. Yu, B. Zhang, W. Feng, and S. Q. Feng, *Appl. Phys. Lett.*, **78**, 407 (2001).
7 J. J. Wu and S. C. Liu, *Adv. Mater.*, **14**, 215 (2002).
8 Y. W. Wang, L. D. Zhang, G. Z. Wang, X. S. Peng, Z. Q. Chu, and C. H. Liang, *J. Cryst. Growth*, **234**, 171 (2002).
9 Z. W. Pan, Z. R. Dai, and Z. L. Wang, *Science*, **291**, 1947 (2001).
10 B. D. Yao, Y. F. Chan, and N. Wang, *Appl. Phys. Lett.*, **81**, 757 (2002).
11 M. Farnsworth and C. H. Kline, *Z. Chem.*, **1973**, 47.
12 K. Vanheusden, W. L. Warren, C. H. Seager, D. K. Tallant, J. A. Voigt, and B. E. Gnade, *J. Appl. Phys.*, **79**, 7983 (1996).

Published on the web (Advance View) May 27, 2003; DOI 10.1246/cl.2003.546